The Dynein Stalk Contains an Antiparallel Coiled Coil with Region-Specific Stability[†]

Peter Höök,[‡] Toshiki Yagi,[‡,§] Anindya Ghosh-Roy,[‡,||] John C. Williams,[⊥] and Richard B. Vallee*[,‡]

Department of Pathology and Cell Biology, Columbia University, New York, New York 10032, Department of Biochemistry and Molecular Biology, Thomas Jefferson University, Philadelphia, Pennsylvania 19107, and Department of Molecular Medicine, Beckman Research Institute of the City of Hope, Duarte, California 91010

Received February 10, 2009; Revised Manuscript Received February 13, 2009

ABSTRACT: The dynein motor proteins interact with microtubules at the distal end of an unusual 12−15 nm stalk, which communicates with the sites for nucleotide hydrolysis and microtubule binding in a cyclical, bidirectional manner. Here, we report that the stalk shaft of rat cytoplasmic dynein is an antiparallel α-helical coiled coil, the stability of which is markedly altered by changes at its proximal and distal ends, consistent with a structure capable of rapid, cyclical rearrangement during the dynein cross-bridge cycle.

The dyneins are retrograde microtubule motor proteins involved in axonemal and cytoplasmic functions. Cytoplasmic dynein is alone involved in a very wide range of functions, including vesicular and macromolecular transport, chromosome movement, nucleus positioning, and cell migration (*1*). Cytoplasmic dynein contains two motor domains, each of which consists of a ringlike structure of six covalently linked AAA domains (*2*) from which two extended structures project, the tail, which is involved in dimerization and cargo binding, and the stalk, an elongated structure consisting of a thin shaft with a small globular microtubule-binding domain (MTBD) at its tip (*3*). Binding and release of dynein from the microtubule surface are regulated by nucleotide hydrolysis primarily in the first and third AAA domains (*4*−*6*). Conversely, microtubule binding stimulates ADP release (*7*), the rate-limiting step in the dynein mechanochemical cycle (*8*), suggesting that the stalk must serve to communicate information in a bidirectional, cyclical manner.

The shaft of the stalk has been proposed to consist of an ∼12−15 nm long α-helical coiled coil, on the basis of secondary structure prediction and electron microscopy analysis (*3, 9, 10*). A shift in register of the coiled coil α-helices was recently proposed as the underlying mechanism by which the dynein stalk modulates its microtubule affinity (*11*). Such reorganization within the stabilizing hydrophobic core of the coiled coil, however, may be energetically unfavorable and would likely require an imperfect packing of the α-helical interface.

This study was initiated to test directly for α-helical coiled coil structure within the stalk and to understand the basis for conformational flexibility. We find that the stalk shaft is almost completely α-helical and acts as an antiparallel coiled coil in cross-linking analysis. Mutational analysis reveals an important role for both the proximal and distal regions of the shaft, as well as the microtubule-binding domain, in coiled coil stability. In all, the results from this study provide novel insight into the structural dynamics of the dynein stalk.

MATERIALS AND METHODS

Protein Production. DNA of stalk fragments was amplified by PCR from the recombinant rat cytoplasmic dynein motor domain fragment (*7*) and cloned into pGEX-2T bacterial cell expression vector (GE Healthcare) using BamHI and EcoRI restriction sites. Transformed *Escherichia coli* strain BL21(DE3) was grown at 37 °C until an A_{600} of ∼0.5 was reached. Protein expression was induced with 0.5 mM IPTG[1] for 18−20 h at 20 °C. Expressed protein was extracted by sonication in phosphate-buffered saline (PBS). Clarified lysate was applied on a GST SpinTrap purification column (GE Healthcare). Unbound material was removed when the sample was washed with PBS, and GST-fused protein was eluted with 10 mM glutathione. Eluted protein was extensively dialyzed in PBS to remove the glutathione. Thrombin (Calbiochem) was used to remove GST by cleavage at a site located immediately upstream from the BamHI restriction site. The sample was applied to a GST SpinTrap purification column to remove the GST. The purity of the stalk fragment was analyzed by SDS−PAGE.

Site-Directed Mutagenesis and Detection of Cross-Linked Cysteine Residues. Cysteine and alanine residues were introduced by site-directed mutagenesis (QuickChange II; Stratagene). Disulfide formation occurred spontaneously by

[†] This study was supported by a Muscular Dystrophy Association Research Development Grant.

* To whom correspondence should be addressed. Phone: (212) 342-0546. Fax: (212) 305-5498. E-mail: rv2025@columbia.edu.

[‡] Columbia University.

[§] Present address: Graduate School of Science, Kyoto University, Kyoto, Japan.

[||] Present address: Section of Neurobiology, Division of Biological Sciences, University of California at San Diego, La Jolla, CA 92093.

[⊥] Thomas Jefferson University and Beckman Research Institute of the City of Hope.

[1] Abbreviations: CD, circular dichroism; IPTG, isopropyl β-D-thiogalactoside; GST, glutathione *S*-transferase; PBS, phosphate-buffered saline; Pipes, 1,4-piperazinediethanesulfonic acid; SDS−PAGE, sodium dodecyl sulfate−polyacrylamide electrophoresis.

10.1021/bi900223x CCC: $40.75
Published on Web 02/17/2009

air oxidation. Cysteine disulfide formation was assessed by a faster electrophoretic mobility of the oxidized protein versus that of the reduced protein on SDS−PAGE.

Circular Dichroism (CD) Spectroscopy. CD spectra were recorded from the average of three scans taken with a bandwidth of 1 nm over a spectral range of 200−280 nm with a 4 s response time and at 100 nm/min on a Jasco J-810 spectropolarimeter (Jasco, Inc.). Melting scans were performed at 220 nm over a temperature range of 15−80 °C; data were collected in 1 °C increments at 40 °C/h, and refolding was assessed when the sample was cooled to 15 °C at the same rate. The transition midpoint temperature, T_m, was defined as the temperature at which there is a 50% decrease in molar ellipticity compared with that at 15 and 80 °C. The total protein concentration was 10 μM in PBS as determined from the absorbance at 280 nm.

Identification of Proteolytic Fragments. Proteomic analysis of stalk fragments was conducted at the Columbia University Protein Core Facility. N-Terminal sequencing was carried out on electroblotted proteolytic fragments by automated Edman degradation on a 494 protein sequencer (Applied Biosystems) and by high-pressure liquid chromatography. The C-terminal boundaries were deduced by measuring the masses of the proteolytic fragments using matrix-assisted laser desorption ionization time-of-flight mass spectrometry. Spectra were acquired on a Voyager-DE Pro instrument (Applied Biosystems) operating in linear mode.

Microtubule Binding Assay. To facilitate analysis of microtubule binding, 5 μM GST-dimerized stalk fragment was incubated for 30 min with 10 μM paclitaxel-stabilized microtubules (tubulin; cytoskeleton) in 10 mM Pipes (pH 7.0) and 2 mM $MgCl_2$ supplemented with 20 μM paclitaxel and pelleted at 130000*g* for 30 min at 25 °C. Pellet and supernatant fractions were analyzed by SDS−PAGE.

RESULTS

Analysis of Stalk Structural Stability. To test directly for α-helical coiled coil structure within the stalk and to understand the basis for conformational flexibility, we prepared a series of stalk constructs. The boundaries of the stalk were based on coiled coil prediction, and by identification of 11 potential consecutive heptad repeats flanking the 125 residues of MTBD (Figure 1A). Two series of constructs were made, one encompassing the entire stalk (Stalk) and another (ΔMTBD) in which the MTBD was replaced by five glycine residues inserted between two completely conserved prolines. The recombinant Stalk and ΔMTBD proteins were very soluble and homogeneous as judged by SDS−PAGE and native-PAGE (Figure 1B).

Far-UV circular dichroism (CD) spectroscopy revealed the Stalk to be 47% α-helical (Figure 2A and Table 1). Strikingly, $[\theta]_{222}$ of ΔMTBD was 35708 deg cm^2 dmol^{-1}, close to the calculated value of 38262 deg cm^2 dmol^{-1} for a helix similar in length (*12*). The $[\theta]_{222}/[\theta]_{208}$ ratio was 1.05, characteristic of an α-helical coiled coil (Figure 2A and Table 1). These results suggest that the stalk shaft is almost entirely in the form of an α-helical coiled coil. Thermal denaturation analysis of Stalk revealed gradual and irreversible loss of helical structure with a single cooperative unfolding at 48 °C (Figure 2B and Table 1). In contrast, ΔMTBD exhibited a three-state denaturation profile with cooperative unfolding

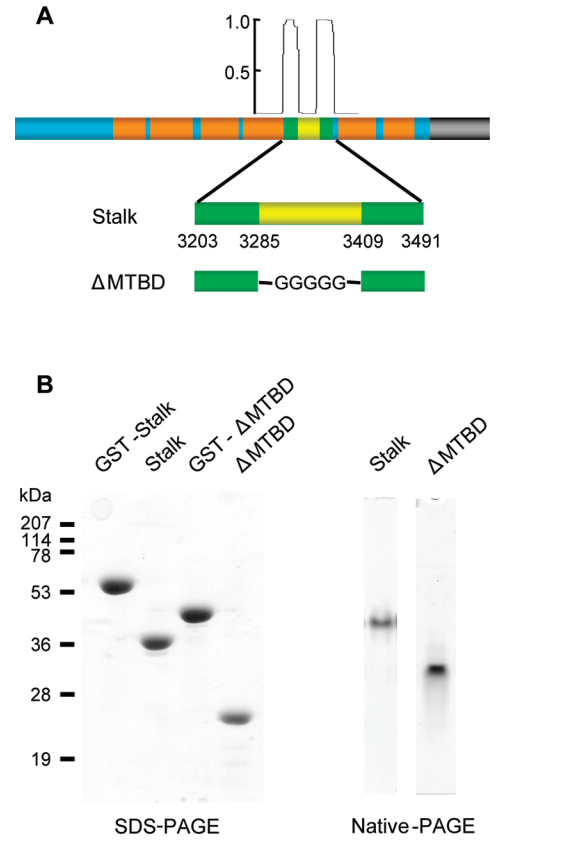

FIGURE 1: (A) Map of the rat cytoplasmic dynein motor domain. The six AAA units are colored red, and the microtubule-binding stalk is colored green and yellow. The top shows the probability for coiled coil formation assessed by the COILS program (*3*). The bottom is a representation of the principal recombinant Stalk and ΔMTBD constructs used in this study, which were further modified as described. The N- and C-terminal boundaries for Stalk, ΔMTBD, and the MTBD are indicated. (B) Electrophoresis of stalk constructs under denaturing (left) and native (right) conditions.

at 30 and 52 °C (Figure 2C and Table 1), consistent with regions of differing stability. We observe that 48% of the helical structure was denatured at 37 °C, indicative of relatively weak coiled coil structure. Refolding was virtually without hysteresis, in contrast to Stalk, which showed almost no evidence of α-helical refolding.

To test the relative orientation of the α-helices, cysteine residues were introduced at the Stalk N- and C-termini (Stalk^{cc}) or two heptads from the termini (Stalk^{c2c2}). Analysis by nonreducing SDS−PAGE showed a marked increase in electrophoretic mobility, which was reversed by β-mercaptoethanol (Figure 3A). This reaction occurred readily without the need for an oxidizing agent. Similar behavior was observed for ΔMTBD^{cc} and ΔMTBD^{c2c2} (Figure 3B). Disulfide formation in the Stalk constructs increased the α-helical content to 60% (Table 1). Together, these observations strongly support an antiparallel coiled coil model.

Effects of Proximal and Distal Deletions of the Stalk Coiled Coil Shaft. To assess which regions of the coiled coil are important for its stability, we engineered a series of paired N- and C-terminal truncations with terminal cysteines to test for disulfide formation. Stalk truncated by two heptads (StalkProxΔ2Δ2^{cc}) was still able to undergo disulfide cross-linking. Shortening the Stalk by three (StalkProxΔ3Δ3^{cc}) or four heptads (StalkProxΔ4Δ4^{cc}), however, prevented disulfide formation (Table 1). Comparable results were obtained

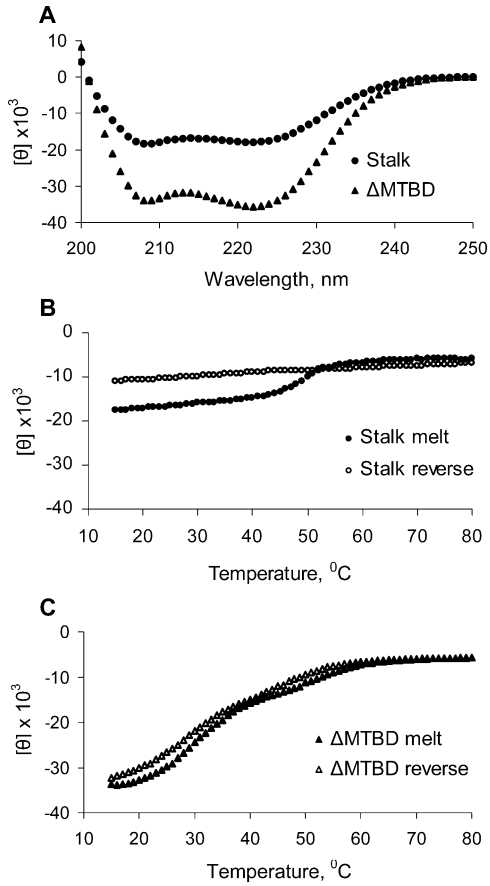

FIGURE 2: (A) CD spectra of Stalk and ΔMTBD. Thermodynamic analysis of Stalk (B) and ΔMTBD (C). The molar ellipticity at 222 nm was monitored as a function of increasing (melt) and decreasing (reverse) temperature.

Table 1: Characterization of Various Stalk Fragments by Disulfide Cross-Linking and Circular Dichroism Spectroscopy

stalk fragment	cross-links	$[\theta]_{222}$ ($\times 10^3$ deg cm^2 dmol^{-1})	α-helix (%)[a]	$[\theta]_{222}/[\theta]_{208}$	T_m (°C)
Stalk	not available	−18.0	47	0.98	48
Stalk^{cc}	yes	−22.9	60	0.99	52
Stalk^{c2c2}	yes				
StalkProxΔ2Δ2^{cc}	yes				
StalkProxΔ3Δ3^{cc}	no				
StalkProxΔ4Δ4^{cc}	no				
Stalk^{cc}K3299A	yes	−12.5	33	0.82	50
ΔMTBD	not available	−35.7	93	1.05	30/50
ΔMTBD^{cc}	yes	−21.2	55	0.98	
ΔMTBD^{c2c2}	yes				
ΔMTBDProxΔ2Δ2^{cc}	yes	−11.5	30	0.92	
ΔMTBDProxΔ3Δ3^{cc}	no	−8.3	22	0.81	
ΔMTBDProxΔ4Δ4^{cc}	no	−13.2	35	1.01	
ΔMTBDDistΔ1Δ1^{cc}	yes	−10.4	27	0.89	
ΔMTBDDistΔ2Δ2^{cc}	yes	−12.3	32	0.90	

[a] The predicted α-helical content is based on the calculated value at $[\theta]_{222}$ for a helix similar in length (*12*).

using truncated and cysteine-substituted ΔMTBD fragments (Table 1). Proximal truncation of ΔMTBD produced a substantial decrease in the level of α-helical secondary structure, with a loss of 70% or more for some of the shorter constructs (Table 1). Removal of one or two heptads from the distal end of ΔMTBD (ΔMTBDDistΔ1Δ1^{cc} and ΔMTBDDistΔ2Δ2^{cc}) led to a similarly severe loss of α-helical structure. Disulfide formation between N- and C-terminal cysteines still occurred in these constructs, suggesting persistence of the proximal region of the stalk

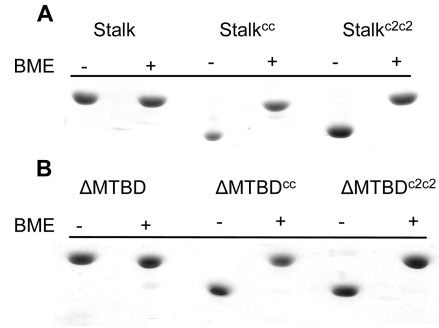

FIGURE 3: Test of disulfide cross-linking between pairs of cysteines introduced at the termini or two heptads from the termini of Stalk (A) and ΔMTBD (B). Disulfide formation was tested by SDS−PAGE in the absence and presence of β-mercaptoethanol (BME). A shift in the position of the electrophoretic band in absence of BME is indicative of disulfide formation. Stalk and ΔMTBD without cysteines are included as controls.

coiled coil. These results argue that the distal and proximal regions of the coiled coil are required for complete folding.

Allosteric Communication. The further possibility of conformational communication between proximal and distal ends of the stalk coiled coil is suggested by other aspects of modified Stalk and shaft behavior. We observed, for example, that proximally truncated Stalk exhibited evidence of autoproteolytic cleavage at a single remote site. The cleavage site was identified by mass spectrometry and mapped C-terminal to a highly conserved lysine pair within the MTBD, suggesting an important role for the proximal region of the shaft in communicating conformational changes within the stalk. To explore the implications for long-range allosteric communication, we replaced one or both lysines with alanine. These mutations abolished proteolytic cleavage but also produced pronounced inhibition of microtubule binding (Figure 4A), analogous to what was reported from in vitro-translated stalk fragments in *Dictyostelium* cytoplasmic dynein (*13*). Surprisingly, however, even the single lysine mutation caused a substantial loss of α-helical coiled coil structure (Figure 4B). Thus, relatively minor changes to the MTBD produce dramatic changes throughout the stalk.

DISCUSSION

Our results provide direct evidence for the relatively unusual antiparallel α-helical coiled coil structure proposed for the dynein stalk. Two features of this coiled coil are noteworthy. First, it is relatively unstable, consistent with its predicted dynamic role during the dynein cross-bridge cycle. Second, the proximal and distal heptads are particularly important for maintaining coiled coil structure. Removal of two heptads either proximally or distally resulted in a relatively severe reduction in α-helical content, and removal of additional heptads resulted in apparent misalignment of terminal cysteines. These effects are consistent with a role for the coiled coil portion of the Stalk in conformational communication between its proximal end and the distal MTBD. The proteolytic sensitivity of the proximally truncated stalk at the conserved lysine pair within the MTBD further supports this possibility. Conversely, mutation of one of the lysines altered the total α-helical content of our stalk constructs, suggesting long-range destabilization of the coiled coil by the single mutation.

A recent X-ray crystallography study reported a high-resolution structure for the distal portion of the dynein stalk

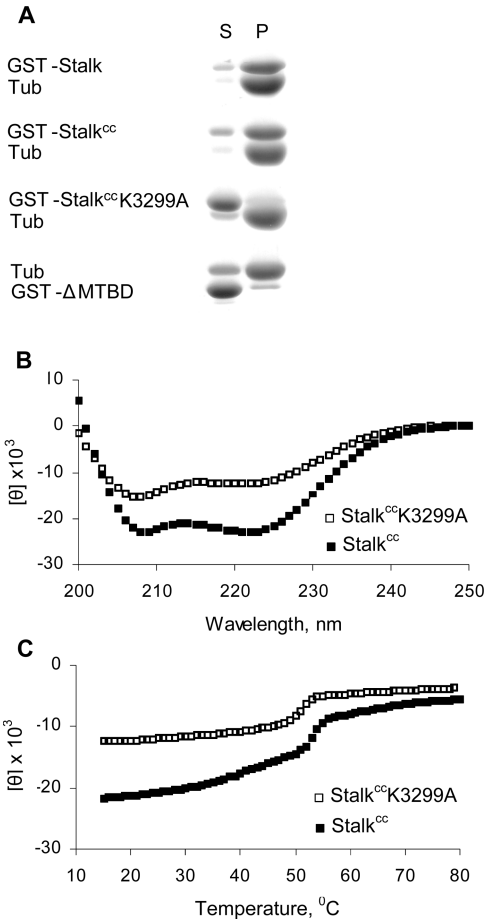

FIGURE 4: (A) Microtubule binding of stalk fragments. SDS−PAGE showing the content of supernatant (S) and pellet (P) fractions from cosedimentation assays of polymerized microtubules (Tub) and various stalk fragments. GST-Stalk and GST-Stalk^{cc} exhibited strong microtubule binding affinity, while minimum microtubule binding was detected for GST-ΔMTBD and GST-Stalk^{cc}K3299A. Effects of Lys^{3299} to Ala^{3299} substitution on Stalk α-helical content (B) and stability (C).

fused to the seryl-t-RNA synthetase antiparallel coiled coil (*14*). The structure included the MTBD and part of the coiled coil region. The conserved lysine pair identified in the study presented here is located at the juncture between the coiled coil and MTBD. Thus, our results suggest that this region is particularly important in communicating conformational changes in the MTBD to the proximal end of the stalk. We also note that mutation of the conserved lysines inhibits stalk microtubule binding (Figure 4A and ref *13*). Although this result is consistent with a direct role for the lysines in microtubule binding, our results raise the possibility that microtubule binding could be affected indirectly through large-scale conformational changes throughout the stalk.

We note that denaturation analysis of lysine-mutated Stalk^{cc} revealed a single, highly cooperative transition at 50 °C, equivalent to that of wild-type Stalk^{cc} (Figure 4C and Table 1). This result and the absence of the cooperative feature in ΔMTBD (Figure 2C) suggest that it corresponds to denaturation of the MTBD, which was reported to be entirely α-helical (*14*). If so, mutation of the conserved lysines may predominantly affect the stability of the stalk.

We note, finally, that ΔMTBD in our analysis is almost entirely α-helical, though Stalk exhibited only 60% α-helical content. Thus, in the complete Stalk produced and characterized in the current study, either the MTBD must be conformationally altered or regions of the coiled coil are disorganized. These considerations raise the possibility of major alterations in stalk α-helical content as dynein progresses through its cross-bridge cycle.

ACKNOWLEDGMENT

We thank Dr. Jennifer Litowski, Dr. Dileep Varma, Shahrnaz Kemal, and Amanda Roberts-Siglin for their assistance and helpful discussions.

REFERENCES

1. Vallee, R. B., Williams, J. C., Varma, D., and Barnhart, L. E. (2004) Dynein: An ancient motor protein involved in multiple modes of transport. *J. Neurobiol. 58*, 189–200.
2. Neuwald, A. F., Aravind, L., Spouge, J. L., and Koonin, E. V. (1999) AAA+: A class of chaperone-like ATPases associated with the assembly, operation, and disassembly of protein complexes. *Genome Res. 9*, 27–43.
3. Gee, M. A., Heuser, J. E., and Vallee, R. B. (1997) An extended microtubule-binding structure within the dynein motor domain. *Nature 390*, 636–639.
4. Silvanovich, A., Li, M., Serr, M., Mische, S., and Hays, T. S. (2003) The third P-loop domain in cytoplasmic dynein heavy chain is essential for dynein motor function and ATP-sensitive microtubule binding. *Mol. Biol. Cell 14*, 1355–1365.
5. Kon, T., Nishiura, M., Ohkura, R., Toyoshima, Y. Y., and Sutoh, K. (2004) Distinct functions of nucleotide-binding/hydrolysis sites in the four AAA modules of cytoplasmic dynein. *Biochemistry 43*, 11266–11274.
6. Reck-Peterson, S. L., and Vale, R. D. (2004) Molecular dissection of the roles of nucleotide binding and hydrolysis in dynein's AAA domains in *Saccharomyces cerevisiae*. *Proc. Natl. Acad. Sci. U.S.A. 101*, 1491–1495.
7. Höök, P., Mikami, A., Shafer, B., Chait, B. T., Rosenfeld, S. S., and Vallee, R. B. (2005) Long range allosteric control of cytoplasmic dynein ATPase activity by the stalk and C-terminal domains. *J. Biol. Chem. 280*, 33045–33054.
8. Holzbaur, E. L., and Johnson, K. A. (1989) ADP release is rate limiting in steady-state turnover by the dynein adenosinetriphosphatase. *Biochemistry 28*, 5577–5585.
9. Burgess, S. A., Walker, M. L., Sakakibara, H., Knight, P. J., and Oiwa, K. (2003) Dynein structure and power stroke. *Nature 421*, 715–718.
10. Mizuno, N., Narita, A., Kon, T., Sutoh, K., and Kikkawa, M. (2007) Three-dimensional structure of cytoplasmic dynein bound to microtubules. *Proc. Natl. Acad. Sci. U.S.A. 104*, 20832–20837.
11. Gibbons, I. R., Garbarino, J. E., Tan, C. E., Reck-Peterson, S. L., Vale, R. D., and Carter, A. P. (2005) The affinity of the dynein microtubule-binding domain is modulated by the conformation of its coiled-coil stalk. *J. Biol. Chem. 280*, 23960–23965.
12. Chen, Y.-H., Yang, J. T., and Chau, K. H. (1974) Determination of the helix and β form of proteins in aqueous solution by circular dichroism. *Biochemistry 13*, 3350–3359.
13. Koonce, M. P., and Tikhonenko, I. (2000) Functional elements within the dynein microtubule-binding domain. *Mol. Biol. Cell 11*, 523–529.
14. Carter, A. P., Garbarino, J. E., Wilson-Kubalek, E. M., Shipley, W. E., Cho, C., Milligan, R. A., Vale, R. D., and Gibbons, I. R. (2008) Structure and functional role of dynein's microtubule-binding domain. *Science 322*, 1691–1695.

BI900223X